PHYSICAL REVIEW B

CONDENSED MATTER

THIRD SERIES, VOLUME 47, NUMBER 17 1 MAY 1993-I

Determination of all elastic constants of transversely isotropic media with a cusp around the symmetric axis by use of elastic pulses propagating in two principal directions

Kwang Yul Kim and Wolfgang Sachse

Department of Theoretical and Applied Mechanics, Cornell University, Ithaca, New York 14853

(Received 14 September 1992)

This paper describes a method of determining all five elastic constants of a hexagonal or transversely isotropic medium of type II which has the cuspidal region of group velocity around the highest-symmetry axis [001] perpendicular to the transversely isotropic basal plane. The elastic constants are obtained from wave-speed data of broad-band ultrasonic signals propagating in two principal directions, namely the [001] and the other parallel to the basal plane. The method uses specific cuspidal features of the slow transverse (ST) mode propagating in the [001] direction with two distinct group velocities. An analytic formula that relates the slower group velocity of the ST mode with the elastic constant C_{13} is derived. An example is provided with a single crystal of zinc exhibiting hexagonal symmetry. The advantages of this method lie in both its simplicity for implementation and its improved accuracy for determination of the elastic constant C_{13}.

I. INTRODUCTION

The theory of plane waves of sound propagating through nondissipative media, including those of hexagonal or transversely isotropic symmetry, have been excellently described by several authors.[1-4] Spherical waves emanating from the monopolar and dipolar point sources and propagating in every direction of isotropic media have been explained by others.[5-7] Measurements of the speed of these sound waves made by adopting various techniques that use either harmonic waves or broadband pulses can be found elsewhere.[8-10]

For the most convenient and precise determination of the elastic constant, the waves propagating in the directions of principal symmetry axes of media have been used for several reasons: first, these directions can be easily found or identified with best accuracy through macroscopic or microscopic observations or through an x-ray analysis; second, in these directions samples of single-crystalline form can be easily grown, cut, and aligned by means of cleavage or favorable chemical etching, and this facilitates a preparation for samples with uniform, parallel, and finely polished surfaces (anisotropic composite materials can also be easily fabricated and machined along these directions); third, because of at least mirror symmetry of material properties across the principal planes of materials with orthorhombic or higher symmetry, variations of wave speed and elastic constants are minimal around the principal directions in comparison with other nonsymmetric directions and thus any errors in elastic constants associated with a small misorientation of the sample about these axes are minimized; finally, most important of all, both phase and group velocities of the broadband elastic pulses propagating in the principal directions coincide with each other and simple formulas relating the speed of both longitudinal and transverse waves to the elastic constants exist. This allows us to determine all the elastic constants for materials of cubic or isotropic symmetry. However, for materials with hexagonal (or transversely isotropic), tetragonal, orthorhombic (or orthotropic), or lower symmetries, additional measurements using the waves propagating in the nonprincipal directions are required to determine all the elastic constants. This poses difficulties in sample preparation and results in less overall accuracy in determination of them. Complications arise as to the waves of the nonprincipal directions of the anisotropic media, because wave propagation through them becomes dispersive even in the absence of dissipation, and no simple analytic formula can be found that relates the group velocities with phase velocities from which the elastic constants can be calculated. Although all the elastic moduli can be obtained from the data of group velocities of broadband sound waves propagating in the general directions of anisotropic media by adopting such an elaborate scheme as the iterative nonlinear least-squares method,[11,12] this introduces additional difficulties and errors associated with the elastic constants.

Recently, we investigated the wave propagation in a single crystal of silicon,[13] using a point-source–point-

 ©1993 The American Physical Society

receiver (PS-PR) technique that was particularly well suited for the study of wave propagation in various directions of elastic media. The pointlike-source excitation of broadband sound waves was accomplished by breaking a tiny glass capillary and also by irradiation of a high-intensity, pulsed laser beam focused on the surface of the silicon crystal. Capacitive and piezoelectric transducers with a diameter of about 1 mm were used as pointlike detectors. Of particular interest is the wave propagation through a cuspidal region around a ⟨100⟩ axis of silicon, quite unlike those found in isotropic materials. No theoretical Green's function is available for cubic media, and therefore a direct comparison of our data with theory is not yet possible. However, Payton[14,15] calculated a Green's function G_{33} for a half-space medium of hexagonal zinc, the slowness surface around the [0001] axis of which bears some similarities to that of silicon around a ⟨100⟩ cubic axis. Comparison of the silicon experimental data with Payton's results was quite revealing and illuminating about the nature of the cuspidal features of silicon.

To have a direct comparison of experimental data with Payton's results and to investigate further the wave propagation through the cuspidal region of zinc, we used a zinc single crystal oriented in the [0001] axis perpendicular to the transversely isotropic basal plane. Zinc has the additional advantage that its cuspidal region lies around the [0001] axis (type II), instead of lying somewhere around a nonprincipal direction (type V). Classification of the transversely isotropic media will be described in Sec. II. This paper describes the broadband waves propagating in the [0001] direction with one longitudinal (L) group velocity and two distinct group velocities associated with the slow transverse (ST) waves. The group velocity of the faster branch of the ST (FST) mode is the same as that of the fast transverse (FT) wave and, therefore, the arrival of the FST mode at the detector reveals no new information for determination of an elastic constant. However, the slower branch of the ST (SST) mode is highly focused toward the [0001] direction. As a result, its arrival is very much pronounced and easily identified as a minimum point of a deep trough in the signal detected by a capacitive transducer. The easy identification of the SST-mode arrival enables us to calculate with minimum error its group velocity, which is directly related to the elastic constant by an analytical formula derived from the ST sheet of the slowness surface of zinc. This, combined with other velocity data of waves propagating in two principal directions and measured by the conventional techniques, yields all five elastic constants of zinc.

II. THEORY

A. Wave surfaces

The following treatment of the wave surfaces, such as those of phase and group velocities, and of the slowness of elastic waves, has been extensively given in Refs. 2–4. In brief, let indices 1 and 2 of the reference coordinate system be any of two mutually perpendicular axes lying in the transversely isotropic basal plane; the direction of index 3 represents the axis of circular symmetry, perpendicular to the basal plane. Then, the fourth-rank elastic stiffness tensor C_{ijkl} of a hexagonal or transversely isotropic medium is characterized by five constants, $C_{11}=C_{22}$, C_{33}, $C_{44}=C_{55}$, C_{12}, $C_{13}=C_{23}$, for which the identity $C_{66}=\frac{1}{2}(C_{11}-C_{12})$ holds. The phase velocity surface V of the hexagonal system is conveniently written in the forms first given by Christoffel,[2,3]

$$V=\det|\Gamma_{ik}-\rho v^2\delta_{ik}|=0\ , \tag{2.1}$$

where ρ is the density of the sample medium, v is the phase velocity, δ_{ik} represents Kronecker's delta, and Christoffel's stiffness tensor $\Gamma_{ik}\equiv C_{ijkl}n_jn_l$ for the hexagonal medium is defined as

$$\begin{aligned}
\Gamma_{11}&=C_{11}n_1^2+C_{66}n_2^2+C_{44}n_3^2\ ,\\
\Gamma_{22}&=C_{66}n_1^2+C_{11}n_2^2+C_{44}n_3^2\ ,\\
\Gamma_{33}&=C_{44}n_1^2+C_{44}n_2^2+C_{33}n_3^2\ ,\\
\Gamma_{23}&=\Gamma_{32}=n_2n_3(C_{44}+C_{13})\ ,\\
\Gamma_{13}&=\Gamma_{31}=n_1n_3(C_{44}+C_{13})\ ,\\
\Gamma_{12}&=\Gamma_{21}=n_1n_2(C_{66}+C_{12})\ ,
\end{aligned} \tag{2.2}$$

where the unit normal vector $\mathbf{n}$ of the wave is parallel to the wave propagation vector $\mathbf{k}$. Defining the slowness vector $\mathbf{s}$ by the relation

$$s_i\equiv n_i/v\ , \tag{2.3}$$

then the slowness surface S is written as

$$S=\det|C_{ijkl}s_js_l-\rho\delta_{ik}|=0\ . \tag{2.4}$$

Let ω represent the angular frequency. Using the relation

$$v=\omega/k \tag{2.5}$$

and Eq. (2.1), one obtains the wave-vector surface Ω given by

$$\Omega=\det|k^2\Gamma_{ik}-\rho\omega^2\delta_{ik}|=0\ , \tag{2.6}$$

where k is the magnitude of the propagation vector $\mathbf{k}$. The group velocity ξ, usually defined by the relation

$$\xi\equiv\nabla_{\mathbf{k}}\omega=-\frac{\nabla_{\mathbf{k}}\Omega}{\partial\Omega/\partial\omega}\ , \tag{2.7}$$

can also be calculated from Eqs. (2.1), and (2.4), using

$$\xi=\nabla_{\mathbf{n}}v=-\frac{\nabla_{\mathbf{n}}V}{\partial V/\partial v}=\frac{\nabla_{\mathbf{s}}S}{\mathbf{s}\cdot\nabla_{\mathbf{s}}S}\ . \tag{2.8}$$

A convenient way of obtaining these surfaces is to construct the slowness surface, from which one then proceeds to find the surfaces of phase and group velocities, using Eq. (2.3) and the last part of Eq. (2.8). The specimen used in our experiment is a [0001] oriented, hexagonal zinc single crystal. Considering other transversely isotropic materials, such as uniaxially aligned, fiber reinforced composites, we henceforth do not distin-

guish the [0001] crystallographic notation of hexagonal media from the [001] notation used for composites, which we will use to represent the third axial direction perpendicular to the basal plane. Because of the circular symmetry of the above-mentioned surfaces of zinc about the [001] direction, we choose, without loss of generality, a (010) zonal section normal to the basal plane and perpendicular to the [010] direction to represent these surfaces.

Our measured values of elastic constants, virtually identical with those obtained by Alers and Neighbours,[16] were used to generate a (010) section of slowness surface, shown in Fig. 1, and the corresponding sections of the surfaces of phase and group velocities, plotted in Fig. 2 with dotted and solid lines, respectively. As shown in these figures, each surface consists of three sheets, one corresponding to the longitudinal (L) wave, the other two corresponding to the fast transverse (FT) and the slow transverse (ST) waves. Of these waves, only the FT wave is, for every direction of propagation in the zonal section, of pure mode, the polarization of which is of the SH (shear horizontal) type perpendicular to the sagittal plane identical with the zonal section. In a general direction of propagation, L and ST waves are, respectively, quasilongitudinal and quasitransverse, polarized in the sagittal plane, where the polarization of the ST mode is simply described as SV (shear vertical). Both L and ST waves become of pure mode for the waves with **k** directed either in the [001] or in the basal plane.

For these waves of pure mode, the group velocity is equal to the phase velocity, and simple equations relating these velocities to the elastic constants of the medium can be found. For waves propagating parallel to the basal plane, the relations are

$$C_{11}=\rho v_L^2 \ , \quad (L \text{ mode}) \ , \tag{2.9}$$

$$C_{44}=\rho v_{\mathrm{ST}}^2 \ , \quad (\mathrm{ST} \text{ mode}) \ , \tag{2.10}$$

$$C_{66}=(C_{11}-C_{12})/2=\rho v_{\mathrm{FT}}^2 \ , \quad (\mathrm{FT} \text{ mode}) \ . \tag{2.11}$$

The ST mode of Eq. (2.10) is polarized in the [001] direction, and the FT mode of Eq. (2.11) is polarized in the direction perpendicular to the zonal section. Both modes are considered of SH type in this particular case.

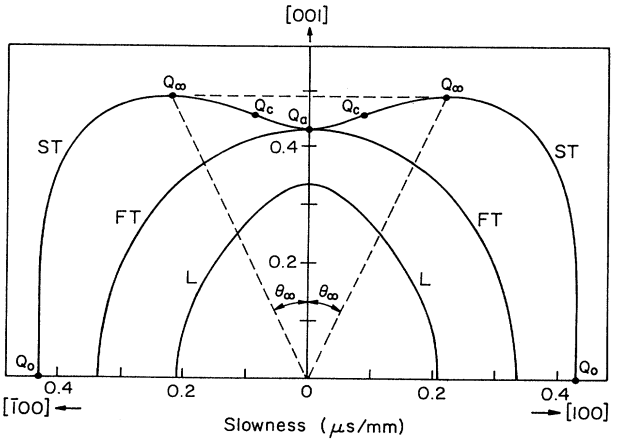

FIG. 1. (010) section of slowness surface of zinc.

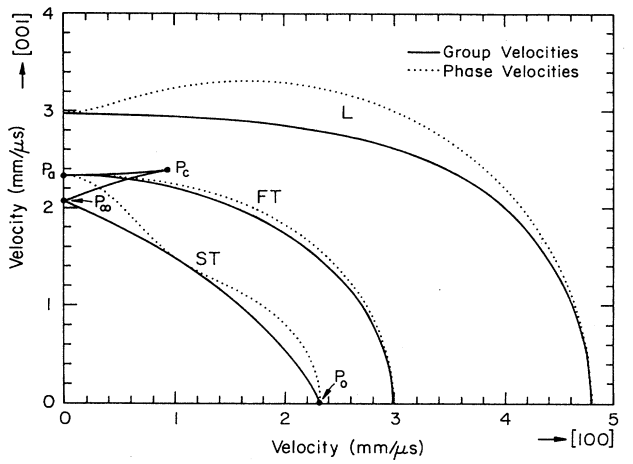

FIG. 2. (010) section of surfaces of phase and group velocities of zinc.

For the waves propagating along the [001] direction, one finds

$$C_{33}=\rho v_L^2 \ , \quad (L \text{ mode}) \ , \tag{2.12}$$

$$C_{44}=\rho v_{\mathrm{T}}^2 \ , \quad (\mathrm{FT} \text{ and } \mathrm{FST} \text{ modes}) \ . \tag{2.13}$$

In this case, the FT mode is degenerate with the faster mode of the ST wave (FST), as indicated in Figs. 1 and 2, where one sees around the [001] direction complicated cuspidal features of the group velocity of the ST mode with two distinct velocities in the [001] direction and with three distinct velocities in the neighborhood of the [001] direction.

The cuspidal features about some specific direction of transversely isotropic media arise due to the particular shape of the slowness surface around that direction. For zinc, the slowness surface of the ST mode about the [001] direction shows a concave sheet, initially concave upward starting from point Q_a, changing its curvature at point Q_c, becoming convex downward with its gradient pointing in the [001] at point Q_∞, and finally reaching point Q_0 at the basal plane. The corresponding points in the group-velocity sheet are marked with P_a, P_c, P_∞, and P_0, respectively. For simplicity of nomenclature, let us call the ray branches of the ST mode, P_aP_c, P_cP_∞, and $P_\infty P_0$, by their acronyms, FST (faster ST) mode, IST (intermediate ST) mode, and SST (slower ST) mode, respectively. All the ST modes with their **k** vectors lying on the conical section OQ_∞ on the slowness surface are focused onto the conical point P_∞ with their rays directed in the [001] direction. Buchwald[17] classified the hexagonal media with the cuspidal features around the [001] axis, like those of zinc, as type-III media. Later, Payton[14] elaborated the category of transversely isotropic media, classifying them into five types according to the locations of the cusps on the ray surface: type I has no cusps; type II has two cuspidal triangles centered on the symmetric

[001] axis; type III has two cuspidal triangles centered on the axis parallel to the basal plane; type IV has four cuspidal triangles centered both on the [001] axis and on the axis parallel to the basal plane; type V has four cuspidal triangles, none of which crosses the coordinate axes. Type IV may be considered as belonging to a subgroup of either type II or type III. Since this paper deals primarily with the wave propagation along the [001] axis that has the cuspidal triangles around it, we henceforth treat type IV as a subgroup of type II. Types I, III, and V will not be discussed further due to their irrelevancy to the investigation of this paper. The condition for being type II is, according to Refs. 2 and 17,

$$(C_{13}+C_{44})^2 > C_{11}(C_{33}-C_{44}) , \tag{2.14}$$

which is of course satisfied for zinc. Other examples of type-II materials are apatite ($Ca_{10}(PO_4)_6F_2$) and cadmium.

B. Determination of the elastic constant C_{13}

For waves traveling along the two principal directions, Eqs. (2.9)–(2.13) yield only four elastic constants C_{11}, C_{33}, C_{44}, and C_{12}. An additional way has to be found to determine C_{13}, which has been usually obtained by measuring the phase velocity of the harmonic L or ST wave propagating in the zonal section with its $\mathbf{k}$ oriented at angle θ from the [001] axis. In this case, the phase velocity is related to the elastic constants by[2,3]

$$\begin{aligned} 2\rho v_{L,\mathrm{ST}}^2 = {} & C_{44}+C_{11}\cos^2\theta+C_{33}\sin^2\theta \\ & \pm[(C_{11}\cos^2\theta-C_{33}\sin^2\theta-C_{44}\cos 2\theta)^2 \\ & +(C_{13}+C_{44})^2\sin^2 2\theta]^{1/2} . \end{aligned} \tag{2.15}$$

In a similar case of using broadband pulses, group velocities are measured that bear no simple analytical relations with the elastic constants. In either case, there arise difficulties associated with sample preparation and accurate orientation in the nonprincipal directions, as mentioned in Sec. II A. This problem, which is associated with the determination of the elastic constant C_{13}, can be circumvented if we generate on the sample a pointlike source of ST broadband pulses having their $\mathbf{k}$ vectors in the direction of OQ_∞ of the slowness surface and propagating along the [001] direction with their group velocities equal to the value of OP_∞ in Fig. 2 and if we detect them by a pointlike transducer, which yields a precise value of the group velocity, because a simple analytical formula can be derived that relates the group velocity OP_∞ of the ST mode with the elastic constant C_{13}. Such excitations of broadband sources of sound waves are possible, for example, with the fracture of a tiny glass capillary and the irradiation of a pulsed laser beam focused on the surface of the sample. A miniature capacitive displacement transducer, described elsewhere,[18] can be used as a pointlike detector.

There is no theoretical Green's function presently available, which may be directly applicable to our experimental data. However, Payton's calculation[14] of a Green's function for a half-space medium of zinc oriented in the [001] direction is quite illuminating. He calculated the time dependence of the surface displacement in the [001] direction, caused by a buried force of Heaviside step-time function with magnitude F_3 acting in the same direction at some distance h from the epicentral position of the surface. Figure 3 describes his result of normalized displacement $w_3=4\pi C_{44}hW_3/(\rho F_3)$ as a function of normalized time $\tau=v_T t/h$, where t represents actual time, $v_T=\sqrt{C_{44}/\rho}$ was already defined in Eq. (2.13), and W_3 is the actual displacement in the [001] direction. In Fig. 3, the arrival of the L wave is marked by L, where a sudden step jump in displacement is evident. After the step, it dwindles monotonically to zero at point T_1, which indicates the arrival of the transverse mode. It causes a kink at T_1 and induces a sharp downward displacement, whose amplitude theoretically reaches to $-\infty$ at point T_2, where the arrival of the ST mode reverses the downward motion, resulting in a sharply steep jump in displacement from $-\infty$ to a positive level, as shown in Fig. 3. A vertical, axisymmetric Heaviside step source acting in the [001] direction of zinc gives rise to the waves of both L and ST modes propagating in virtually every direction inside the medium. However, because of axisymmetry of the source, the net result of displacement in the horizontal direction is zero. Thus, the FT mode of SH polarization cannot be generated by axisymmetric sources, which include the transient vertical force and thermoelastic source, both acting on the surface of a specimen; therefore, the wave arriving at T_1 must be a FST ray. The wave arriving at T_2 is a SST ray associated with conical point Q_∞ on the slowness surface. Payton has already explained the arrivals of the L, FST, and SST rays, as mentioned above with Fig. 3. These arguments are strongly supported by the experiment described in Sec. III. Because of Payton's numerical calculation lacking in detailed analysis, it is not understood why the arrivals of the FST and SST rays cause displacements in opposite directions.

At the point Q_∞ of the slowness surface, $\partial S/\partial s_1=\partial S/\partial s_2=0$, and from Eq. (2.8) one obtains for the group velocity ξ_3 corresponding to Q_∞

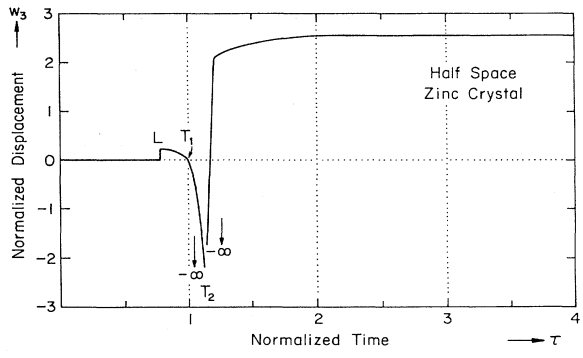

FIG. 3. Displacement response in the [001] direction in zinc due to an excitation of Heaviside step force in the same direction.

$$\xi_3=\frac{1}{s_3}\ , \tag{2.16}$$

where s_3 is the [001]-directional component of slowness s at Q_∞. The value of s_3 can be found from Eqs. (2.2) and (2.4), with the condition that at the point Q_∞ of the slowness surface, $\xi_1=\xi_2=0$ when $s_1\neq 0$ and $s_2\neq 0$. The derivation is straightforward but requires a rather involved process, which will not be described here. Letting

$$A_\pm\equiv C_{11}\pm C_{44}\ , \tag{2.17}$$

$$B_\pm\equiv C_{11}C_{33}\pm C_{44}^2\ , \tag{2.18}$$

$$C\equiv(C_{13}+C_{44})^2\ , \tag{2.19}$$

one finally obtains a quadratic equation for C that only involves the elastic constant C_{13}:

$$C^2-2(B_+-\rho\xi_3^2A_+)C+(B_--\rho\xi_3^2A_-)^2=0\ . \tag{2.20}$$

The above equation, using the measured value of ξ_3 and other known values, determines two positive values of C, the smaller of which fails to meet the condition specified by Eq. (2.14) and is discarded. Thus, Eq. (2.20) yields for C

$$\begin{aligned}C&\equiv(C_{13}+C_{44})^2\\&=C_{11}C_{33}+C_{44}^2-\rho\xi_3^2(C_{11}+C_{44})\\&\quad+2[C_{11}C_{44}(C_{33}-\rho\xi_3^2)(C_{44}-\rho\xi_3^2)]^{1/2}\ ,\end{aligned} \tag{2.21}$$

where the positive square root of C is again chosen for determination of $(C_{13}+C_{44})$, because the negative square root of it yields a large negative value of C_{13}, which usually fails to satisfy one of the thermodynamic conditions for the positive definiteness of strain energy of a hexagonal crystal.[19] These conditions are specified as

$$(C_{11}+C_{12})C_{33}>2C_{13}^2 \quad\text{and}\quad C_{11}C_{33}>C_{13}^2\ . \tag{2.22}$$

Section III will be mainly devoted to how to measure ξ_3 and other elastic constants.

III. EXPERIMENT

A disk-shaped sample of single-crystal zinc oriented in the [001] direction had a basal plane with diameter of about 75 mm, and was about 25.71 mm thick. It was prepared with both top and bottom basal planes polished and parallel to each other. The orientation in the [001] direction was achieved within 0.5° by using an x-ray diffraction pattern. It was observed that a finer adjustment of orientation could be achieved through utilizing the symmetric property of propagation of sound waves about the [001] direction of zinc. A sketch of the sample geometry and the location of sound source and receiver is shown in Fig. 4. Two small portions of the opposite sidewalls perpendicular to the basal plane were made flat, polished, and parallel to each other. The flat faces on the sidewall belong to the zonal section of zinc and were constructed to attach flat broadband piezoelectric transducers of cylindrical shape with about 10 mm diameter. These transducers transmitted either longitudinal or transverse waves in the direction perpendicular to the zonal section. The same piezoelectric transducers were attached on the top surface to generate the broadband plane-wave pulses in the [001] direction. For each measurement, one transducer was used both to transmit the waves and to receive a train of echoes that made a series of round-trips between the parallel faces. These signals were amplified, digitized at a sampling rate of 60 MHz, and displayed on a x-y scope. The round-trip time of the longitudinal and transverse waves was determined by measuring the time interval between the corresponding points of the echoes to calculate their group velocities, which yield four elastic constants C_{11}, C_{33}, C_{44}, and C_{12}, according to Eqs. (2.9)–(2.13). A detailed description of this technique is found in Ref. 10, and we omit further description of it here. It is, however, noted that the plane shear wave transducer mounted on the surface of a specimen generates a transverse mode of SH type, whose polarization is parallel to the attached surface of the sample, and therefore it measures essentially the speed of the FT mode. The ST mode specified by Eq. (2.10) is a special case of SV polarization that becomes parallel to the surface of a zonal section, and this mode can be generated by a shear transducer attached on the flattened sidewall with its polarization aligned in the [001] direction. It is also pointed out that the transverse wave generated by the shear transducer attached on the sidewall with its polarization oriented in an arbitrary direction of the zonal section is split into the two modes specified by Eq. (2.10) and (2.11), facilitating the determination of both C_{44} and C_{66} by a single measurement.

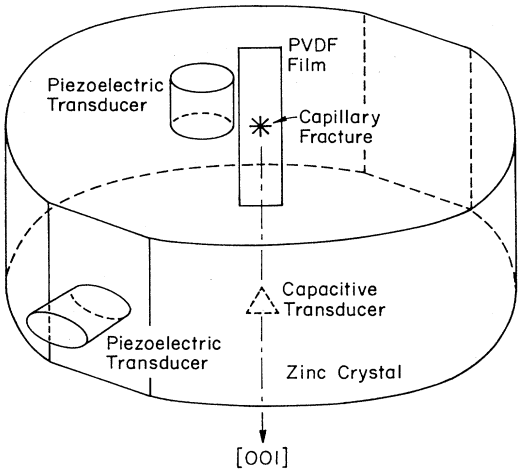

FIG. 4. Geometry of a specimen, the source, and detector for sound waves.

As mentioned earlier, the determination of the elastic constant C_{13} was carried out by using a pointlike source and pointlike receiver (PS-PR) method. The pointlike source of sound waves was generated by breaking a glass capillary of about 0.1 mm size by pressing it vertically with a razor blade at the middle portion of the top sur-

face of the zinc specimen through a piezoelectric polyvinylidene fluoride (PVDF) film with thickness of about 0.08 mm, laid on the top surface of zinc. The output of the PVDF film, generated at a time of capillary fracture, served as a trigger to a digitizer, which sampled at a rate of 60 MHz the amplified output of a capacitive transducer attached on the bottom surface. It also indicated a time of source excitation, which provided a time of reference for measurements of travel times of various rays propagating in the specimen from the top surface to the bottom surface. It was observed that the capillary fracture source[20] resembles a Heaviside step function of force drop with rise time less than 0.1 μs. The magnitude of force drop at the time of the capillary fracture was measured via a miniature load cell attached to the razor blade, and ranged typically from 5 N to 10 N. The capillary fracture generated a broadband sound wave with every possible direction of $\mathbf{k}$ in the medium. As pointed out in Sec. II, because of its axisymmetry, it generated only L and ST modes, whereas the FT mode was absent. The ST mode gave rise to the branches of FST, IST, and SST rays in the cuspidal region of zinc, and in the [001] direction it propagated with two distinct group velocities, those of FST and SST. The signal generated by the capillary fracture traveled through the sample in the [001] direction and was detected by a miniature capacitive displacement transducer with 1 mm diameter. The size of the capacitive transducer subtended a half-conical angle of about 1° when viewed from the capillary source, and the errors associated with this finite aperture of the transducer in determination of elastic constants was negligible in the [001] direction. Such an error becomes gradually larger, as the source-to-receiver orientation moves further away from the [001] direction. The output of the capacitive transducer was amplified by a charge amplifier having a charge-to-voltage conversion factor of 0.25 V/pC and a bandwidth of 10 kHz to 10 MHz. The output of the charge amplifier was connected to the digitizer operating at a 60-MHz sampling rate and displayed on the x-y scope. A detailed description of the miniature capacitive transducer has been given by Kim *et al.*[18] This PS-PR technique was not pursued further along the direction parallel to the basal plane, primarily because it yielded no new information about an elastic constant and partly because no theoretical Green's function G_{11}, to which the experimental data could be compared, was available.

IV. EXPERIMENTAL RESULTS AND DISCUSSION

Four adiabatic elastic constants C_{11}, C_{33}, C_{44}, and C_{12}, obtained by using the plane waves traveling along the two principal directions, are listed in Table I, together with those reported by others.[16,21] They are in excellent agreement with the elastic constants measured by Alers and Neighbours[16] using an ultrasonic pulse-echo technique, and favorably compare with those reported in Ref. 21. The density of zinc[22] used for the calculation of the elastic constants was 7134 kg/m^3.

Figure 5 displays a signal detected by the capacitive transducer. Note a striking similarity between the two

TABLE I. Elastic constants of zinc reported by various authors (in GPa).

Reference	C_{11}	C_{33}	C_{44}	C_{12}	C_{13}
This work	163.75	62.93	38.68	36.28	52.48
Ref. 17	163.68	63.47	38.79	36.40	53.00
Ref. 22	165	61.8	39.6	31.1	50.0

signals shown in Figs. 3 and 5, despite the fact that the experimental signal corresponds to a plate Green's function, instead of a Green's function of a half-space medium. This is not surprising, because the source and receiver in Payton's original calculation of the Green's function of a half-space medium can be interchanged by means of Betti's reciprocal theorem (see Refs. 5 and 6 for a proof of the theorem), and the plate Green's function is directly related to that of a half space via the reflection coefficient of the free surface (001), which has otherwise (or in continuum) a mirror symmetry across it. Therefore, the wave form of the plate Green's function is expected to be similar to that of the half space except for an amplitude. Note that a strong similarity has also been observed for isotropic media under the same circumstances.[5–7] In Fig. 5, L marks the arrival of the longitudinal mode. T_f, which indicates a point of zero crossing after the arrival of the L wave, announces the arrival of the FST branch of the group velocity of the ST mode. The zero crossing in Fig. 5 is observed to be smooth without a kink, as shown in Fig. 3. It is probably because the kink shown in Fig. 3 is not sharp, and in the experimental signal it becomes smoothed due to the finite rise time of the source, finite aperture of the detector, and finite bandwidth of the detection system. More supporting evidence for the interpretation of zero crossing after the L-mode arrival as the arrival of the FST ray has been found in the signals obtained, when the source-to-detector orientation in the zonal section moves from the

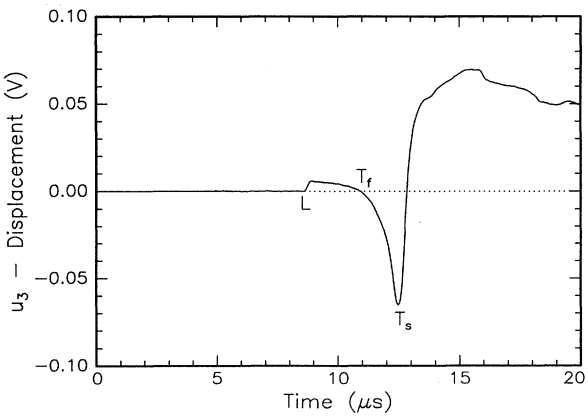

FIG. 5. Displacement signal detected by the capacitive transducer with a zinc specimen with a capillary fracture source. The source-to-detector orientation is in the [001] direction of zinc.

[001] and passes through the cuspidal region. The zero crossing disappears when the propagation direction moves out of the cuspidal region, and the amplitude of the signal remains positive for quite a long time after the arrival of the L mode, leaving the identification of arrivals of only L and SST rays possible. When the propagation direction corresponds with the cuspidal point P_c in Fig. 2, the amplitude of the signal after the L-mode arrival first decreases to zero and then goes positive. The experimental determination of cuspidal curves of the ST mode, including FST, IST, and SST branches, will be published elsewhere.[23] The values of the elastic constants C_{33} and C_{44} calculated according to Eqs. (2.12) and (2.13), using the arrival times of both the L mode and the FST rays in Fig. 5, are found to be virtually identical with those measured by the plane-wave technique.

The point of sharp minimum of a deep trough, marked with T_s in Fig. 5, after the zero crossing would be even more negative if a measurement system of source and detection with higher bandwidth were used. The point T_s corresponds to a point of negative singularity in Fig. 3 and indicates the arrival of the SST branch of the group velocity. This point corresponds to the ST modes having their $\mathbf{k}$'s parallel to the various directions of OQ_∞ with a constant azimuthal angle θ_∞ on the conical section of the slowness surface. The group velocity ξ_3 obtained from the arrival of the SST ray is equal to 2060 m/s. Using $\xi_3 = 2060$ m/s and the known values of the density and all the other elastic constants, one finally determines the elastic constant C_{13} from Eq. (2.21). The value of C_{13} is 52.48 GPa or 16.42 GPa. The $C_{13} = 52.48$ GPa is chosen because it only satisfies the condition of type II specified by Eq. (2.14). Again, this value of C_{13} is in excellent agreement with that of Ref. 16 and in fair agreement with that of Ref. 21. It is emphasized that locating the point T_s in the signal is facilitated due to the nature of sharp minimum; therefore, a very small error is introduced in the determination of C_{13}. This error is expected to be even smaller with a system of higher bandwidth. For the reasons mentioned in Sec. I and above, it is believed that the error associated with C_{13} in our measurement is the smallest among those quoted in Table I.

With all five elastic constants of zinc thus determined, it is pointed out for reference that the azimuthal angle θ_∞ between the [001] axis of zinc and the conical section of OQ_∞ of the slowness surface is calculated to be 24.5°. All those ST modes whose $\mathbf{k}$ vectors lie on the conical surface with the azimuthal angle 24.5° are focused with their ray direction parallel to the [001]. It was observed that the amplitude of the SST ray was maximum in the [001] direction, as predicted by the theory of phonon focusing.[24] This gives strong evidence for the existence of external conical refraction, a phenomenon not observed in acoustics as yet, but claimed to be observed in optics.[25] When this ray transmits through a boundary to an isotropic medium, it gives rise to the external conical refraction, which will be reported elsewhere.[23]

The longitudinal waves propagating along the free surface radiate their energy into the interior to meet the free boundary conditions, and the wave front of these interior rays is known as a head wave. For zinc with a capillary fracture source on the surface, the rays of head waves detected by an epicentral detector constitute a cone centered on the [001] axis with an azimuthal angle 3.04°. The corresponding conical section on the slowness surface has an azimuthal angle 23.3°, slightly less than that of the conical section of OQ_∞ in Fig. 1. The group velocity of the head waves is calculated to be 2113 m/s, and the measured speed of the L wave traveling on the surface equals 4791 m/s. As a result, both the conical head wave and the epicentral SST ray arrive almost simultaneously at the detector. In fact, the arrival of the head wave is calculated to be only 0.0087 μs ahead of the arrival of the SST ray, marked with T_s in Fig. 5 for the zinc specimen with a thickness of 25.705 mm, through which the SST ray takes 12.478 μs to travel. Taking into account the sampling time interval 0.0167 μs and the finite size of the detector (0.5 mm radius), both arrivals are considered as simultaneous within an experimental error. The contribution of the head wave to the epicentral displacement is, however, assumed to be much weaker in comparison with that of the epicentral SST ray, because the axisymmetric capillary fracture source of the L wave propagating along the surface is of dipolar type, whereas the source of the epicentral SST ray is essentially of monopolar type. Rather, the effect of the conical head wave on the epicentral displacement signal could be the broadening of the negative sharp minimum of a deep trough, as shown in Fig. 5, weak and by no means visible as its effect may be in the figure. In contrast, a pulsed laser beam gives rise to a source of dipolar type aligned along the surface and generates a large horizontal surface displacement, which results in the strong L and head waves traveling along the surface and through the interior, respectively. Away from the epicenter, the head wave propagating toward the detector is no longer conic, and its arrival splits apart from that of the SST ray. When a focused pulsed laser beam was scanned on the surface of the zinc specimen, various wave fronts, such as those of the L ray, head waves, and IST and SST rays, were observed to be quite distinctive.[23]

Other interesting questions may be raised as to whether or not the method we have described in this paper is applicable for the determination of elastic constants to other symmetries that show cuspidal features about the principal symmetric axis, say, those of silicon about a $\langle 100 \rangle$ axis. The answer is possibly yes, and the investigation using silicon is under way.

V. CONCLUSIONS

This paper shows a novel method for determining all five elastic constants of type-II hexagonal or transversely isotropic media from the speeds of sound waves propagating along two principal directions, namely [001] and any direction perpendicular to it. The method is demonstrated using a single crystal of zinc. The broadband sound waves generated by the fracture of a tiny glass capillary induces three [001]-directional rays propagating at three distinct group velocities, one associated with the L mode and the other two associated with the ST modes. The detected signal shows first an L-wave arrival and then a

zero crossing immediately followed by a sharp minimum of a deep trough. The zero crossing is caused by the arrival of the FST ray whose group velocity is directly related to the elastic constant C_{44}. The point of sharp minimum indicates the arrival of the SST ray whose group velocity is related to the elastic constant C_{13} by an analytical formula derived from the slowness surface of type-II media. We have shown that it is very easy to determine these group velocities from the signal detected by a pointlike capacitive displacement sensor, and this leads to an accurate determination of the elastic constant C_{13}.

ACKNOWLEDGMENTS

We are deeply grateful for the financial support of the Physical Acoustics Division of the Office of Naval Research. We thank B. F. Addis very much for growing a large single crystal of zinc with fine quality. The use of the facilities of the Materials Science Center of Cornell University is also acknowledged.

[1]R. N. Thurston, in *Mechanics of Solids,* edited by C. Truesdell (Springer-Verlag, New York, 1984), Vol. IV.

[2]M. J. P. Musgrave, *Crystal Acoustics* (Holden-Day, San Francisco, 1970).

[3]B. A. Auld, *Acoustic Fields and Waves in Solids,* 2nd ed. (Krieger, Malabar, FL, 1990), Vol. I and Vol. II.

[4]F. I. Fedorov, *Theory of Elastic Waves in Crystals* (Plenum, New York, 1968).

[5]J. D. Achenbach, *Wave Propagation in Elastic Solids* (North-Holland, New York, 1973).

[6]K. Aki and P. G. Richards, *Quantitative Seismology: Theory and Methods* (Freeman, San Francisco, 1980), Vol. I.

[7]A. N. Ceranoglue and Y. H. Pao, J. Appl. Mech. **48**, 125 (1981); **48**, 133 (1981); **48**, 139 (1981).

[8]H. J. McSkimin, in *Physical Acoustics,* edited by W. P. Mason (Academic, New York, 1964), Vol. I, Part A.

[9]D. I. Bolef and J. deKlerk, IEEE Ultrasonic Eng. **UE-10**, 19 (1963).

[10]E. P. Papadakis, in *Physical Acoustics,* edited by W. P. Mason and R. N. Thurston (Academic, New York, 1976), Vol. XII.

[11]B. Castagnede, K. Y. Kim, W. Sachse, and M. O. Thompson, J. Appl. Phys. **70**, 150 (1991).

[12]A. G. Every and W. Sachse, Phys. Rev. B **42**, 8196 (1990).

[13]K. Y. Kim, W. Sachse, and A. G. Every, J. Acoust. Soc. Am. **93**, 1393 (1993).

[14]R. G. Payton, *Elastic Wave Propagation in Transversely Isotropic Media* (Nijhoff, The Hague, 1983).

[15]R. G. Payton, SIAM J. Appl. Math. **40**, 373 (1981).

[16]G. A. Alers and J. R. Neighbours, J. Phys. Chem. Solids **7**, 58 (1958).

[17]V. T. Buchwald, Proc. R. Soc. London, Ser. A **253**, 563 (1959).

[18]K. Y. Kim, L. Niu, B. Castagnede, and W. Sachse, Rev. Sci. Instrum. **60**, 2785 (1989).

[19]G. A. Alers and J. R. Neighbours, J. Appl. Phys. **28**, 1514 (1957).

[20]F. R. Breckenridge, C. E. Tschiegg, and M. Greenspan, J. Acoust. Soc. Am. **57**, 626 (1975).

[21]R. F. S. Hearmon, in *Elastic, Piezoelectric, Pyroelectric, Piezooptic, Electrooptic Constants, and Nonlinear Dielectric Susceptibilities of Crystals,* edited by K. H. Hellwege, Landolt-Börnstein, New Series, Group III, Vol. 11 (Springer-Verlag, New York, 1979).

[22]H. E. Swanson and E. Tatge, in *Standard X-ray Diffraction Powder Patterns,* National Bureau of Standards Circular No. 539 (U.S. GPO, Washington, D.C., 1953), Vol. 1, p. 16.

[23]K. Y. Kim and W. Sachse, in *Proceedings of the IEEE 1992 Ultrasonics Symposium,* Tucson, AZ, 1992, edited by B. R. McAvoy (IEEE, New York, in press).

[24]A. G. Every, Phys. Rev. B **34**, 2852 (1986).

[25]M. Born and E. Wolf, *Principles of Optics,* 6th ed. (Pergamon, New York, 1980).